THE JOURNAL OF BIOLOGICAL CHEMISTRY VOL. 290, NO. 25, pp. 15878–15891, June 19, 2015

Human CHAC1 Protein Degrades Glutathione, and mRNA Induction Is Regulated by the Transcription Factors ATF4 and ATF3 and a Bipartite ATF/CRE Regulatory Element*

Received for publication, December 23, 2014, and in revised form, April 29, 2015 Published, JBC Papers in Press, April 30, 2015, DOI 10.1074/jbc.M114.635144

Rebecca R. Crawford[‡], Eugenia T. Prescott[‡], Charity F. Sylvester[‡], Ashlee N. Higdon[‡], Jixiu Shan[§1], Michael S. Kilberg[§1], and Imran N. Mungrue[‡2]

From the [‡]Department of Pharmacology and Experimental Therapeutics, Louisiana State University Health Sciences Center, New Orleans, Louisiana 70112 and the [§]Department of Biochemistry and Molecular Biology, Shands Cancer Center and Center for Nutritional Sciences, University of Florida College of Medicine, Gainesville, Florida 32610

Background: *CHAC1* is associated with the stress response in atherosclerosis.
Results: ATF4, ATF3, and CEBPβ regulate *CHAC1* transcription. Human CHAC1 protein overexpression depletes glutathione.
Conclusion: CHAC1 is induced following multiple cell stress signals and leads to depletion of glutathione.
Significance: *CHAC1* may be an essential link between stress signaling and the oxidative status of the cell, contributing to multiple diseases.

Using an unbiased systems genetics approach, we previously predicted a role for CHAC1 in the endoplasmic reticulum stress pathway, linked functionally to activating transcription factor 4 (ATF4) following treatment with oxidized phospholipids, a model for atherosclerosis. Mouse and yeast CHAC1 homologs have been shown to degrade glutathione in yeast and a cell-free system. In this report, we further defined the ATF4-*CHAC1* interaction by cloning the human *CHAC1* promoter upstream of a luciferase reporter system for *in vitro* assays in HEK293 and U2OS cells. Mutation and deletion analyses defined two major *cis* DNA elements necessary and sufficient for *CHAC1* promoter-driven luciferase transcription under conditions of ER stress or ATF4 coexpression: the −267 ATF/cAMP response element (CRE) site and a novel −248 ATF/CRE modifier (ACM) element. We also examined the ability of the *CHAC1* ATF/CRE and ACM sequences to bind ATF4 and ATF3 using immunoblot-EMSA and confirmed ATF4, ATF3, and CCAAT/enhancer-binding protein β binding at the human *CHAC1* promoter in the proximity of the ATF/CRE and ACM using ChIP. To further validate the function of CHAC1 in a human cell model, we measured glutathione levels in HEK293 cells with enhanced CHAC1 expression. Overexpression of CHAC1 led to a robust depletion of glutathione, which was alleviated in a CHAC1 catalytic mutant. These results suggest an important role for CHAC1 in oxidative stress and apoptosis with implications for human health and disease.

The endoplasmic reticulum (ER)[3] is a cellular organelle involved in protein maturation, intracellular trafficking, and calcium storage. Perturbation of normal ER function leads to the buildup of unfolded proteins and the activation of an adaptive signaling program, collectively known as the ER stress pathway, or unfolded protein response (1). The ER stress pathway is initiated by activation of three sensors, ATF6, ERN1 (IRE1), and EIF2AK3 (pancreatic EIF2α kinase) (1, 2), that induce protective events to restore ER function or apoptosis when the initiating stimulus cannot be resolved (1–3).

ATF4 maturation is an early event in the ER stress pathway that requires pancreatic EIF2α kinase phosphorylation of the eukaryotic initiation factor EIF2S1 (EIF2α) (4). A widening body of literature supports a role for *ATF4* as a stress-induced gene with important roles in disease. Atf4 is implicated in the development of diabetes (5, 6), accompanies atherosclerosis (7, 8), and plays a critical role in early osteoblast development (5, 9, 10).

ATF4 activity is also regulated by CCAAT/enhancer-binding protein β (CEBPβ), a basic leucine zipper transcription factor that is responsive to ER stress (11). Three isoforms of CEBPβ have been identified: liver-activating protein (LAP, 35 kDa), LAP* (38 kDa), and liver inhibitory protein (LIP, 20 kDa) (12). Generally, during ER stress, LAP helps ATF4 regulate the pro-survival response. However, increases in the concentration of LIP following prolonged ER stress lead to apoptotic signaling (13).

* This work was supported, in whole or in part, by National Institutes of Health Grant HL094709 (to I. N. M.). This work was also supported by NSF-REU Site (Grant 1359140) studentship (to C. F. S.) and Louisiana Board of Regents Fellowship LESQSF(2012-17)-GF-08 (to R. R. C.). The authors declare that they have no conflicts of interest with the contents of this article.
[1] Supported by National Institutes of Health Grants DK92062 and DK94729.
[2] To whom correspondence should be addressed: 1901 Perdido St., MEB 5259, New Orleans, LA 70112. Tel.: 504-568-2236; Fax: 504-568-2361; E-mail: imungr@lsuhsc.edu.

[3] The abbreviations used are: ER, endoplasmic reticulum; CEBP, CCAAT/enhancer-binding protein; LAP, liver-enriched activator protein; LIP, liver-enriched inhibitory protein; ATF, activating transcription factor; CRE, cAMP response element; ACM, activating transcription factor/cAMP response element modifier; CARE, CCAAT enhancer binding protein-activating transcription factor response element; IM, immunoblot; ASNS, asparagine synthetase; MAFF, V-MAF avian musculoponeurotic fibrosarcoma oncogene family, protein F; CHOP, C/EBP homology protein; Th, thapsigargin; Tm, tunicamycin; HisOH, histidinol.

CHAC1 is a proapoptotic ER stress protein downstream of the pancreatic EIF2α kinase-ATF4 pathway (14) that appears to be important for human physiology and disease. Chac1 has γ-glutamyl cyclotransferase activity toward glutathione in yeast and cell-free models (15, 16). Because glutathione is the major intracellular antioxidant (17), CHAC1 may have an important role in the oxidative balance of the cell. Additionally, Chac1 has γ-glutamyl cyclotransferase activity toward Notch during development, thereby regulating neurogenesis (18, 19). These studies have also identified Glu-116 as the catalytic residue in mice (Glu-115 in humans).

We previously identified a particularly close relationship between *CHAC1* and *ATF4* within the ER stress pathway using a dynamic systems genetic approach in a population of human aortic endothelial cell cultures treated with oxidized 1-palmitoyl-2-arachidonyl-*sn*-3-glycero-phosphorylcholine (20). We have also shown that human *CHAC1* is a target for ATF4 using genetic perturbations *in vitro* (14).

This work expands both the regulation and function of CHAC1 in a human cell model. Here a direct relationship between ATF4 and important regulatory elements within the *CHAC1* promoter is identified. Luciferase assays reveal a critical role for a −267 activating transcription factor/cAMP response element (ATF/CRE) in conjunction with a novel −248 element, dubbed ATF/CRE modifier (ACM). Surprisingly, a conserved −209 CEBP-ATF response element (CARE) plays a minor role in the regulation of human *CHAC1* transcription. Luciferase assays, ChIP, and immunoblot (IM)-EMSA reveal important regulatory activities for ATF4, ATF3, and CEBPβ at the *CHAC1* promoter.

Furthermore, this work illustrates the γ-glutamyl cyclotransferase activity of CHAC1 toward glutathione via a conserved catalytic mechanism in human cells that has not been demonstrated previously in human cells. Overexpression of CHAC1 led to a dramatic reduction in cellular glutathione, whereas mutation of the catalytic site (E115Q) abrogated this activity. These data indicate that CHAC1 regulates the oxidative balance in the cell through depletion of glutathione.

Materials and Methods

Cell Culture—HEK293 cells were cultured as described previously (14). HEK293 cells were transfected with plasmid DNAs using Lipofectamine 2000 (Invitrogen) according to the protocols of the manufacturer. U2OS cells were maintained in McCoy's 5A medium supplemented with 10% fetal bovine serum. U2OS cells were transfected with plasmid DNA using Superfect (Qiagen). Complete medium was changed to treatment media (complete medium plus drug) 24 h after transfection. ER stress was induced using tunicamycin (1 μg/ml, 24 h) and thapsigargin (0.3 μM, 24 h or 3 μM, 4 h). Amino acid starvation was induced using histidinol (2 mM, 24 h), which was freshly prepared on the day of use.

Promoter Constructs—A fragment from bacterial artificial chromosome clone G248P8704A5 (Children's Hospital Oakland Research Institute /Bacpac Resource Center; Oakland, CA) was digested with Nhe1 and cloned upstream of a promoterless luciferase reporter gene into pGL3-basic (Promega). PCR with the following primers was used to remove translated sequences downstream and including the proposed ATG, followed by digestion with Xho1 and Spe1 to generate the final 6.9-kb promoter construct as follows: forward, CTCAGGCCTCTGGGAAGGTT; reverse, TCTAGAAGCTTCTCGAGGTGCCTGGCACAGG ATAGGC. A shorter 2.6-kb promoter construct was generated using limiting internal Sac1 digestion and religation. All constructs were sequenced to verify that errors were not introduced by PCR.

Expression Plasmids and Antibodies—The expression plasmid for CHAC1-GFP has been described previously (14). An active site mutation in CHAC1 was created using site-directed mutagenesis to change a glutamate to a glutamine (GAG to CAG). Expression plasmids for CEBPβ and the splice isoforms CEBPβ-LIP only and CEBPβ-LAP only were a gift from Dr. Maria Hatzoglou (13). The ASNS luciferase plasmid has been described previously (21). The ATF4 plasmid was a gift from Dr. Pierre Fafournoux (22). This plasmid does not contain the upstream ORFs and is constitutively active. Plasmid DNAs contained in eukaryotic expression vectors were obtained from Open Biosystems: MAFF (clone ID 3922552), TRIB3 (clone ID 5104452), CREB1 (clone ID 3872792), and CCAAT/enhancer-binding protein γ (CEBPG) (clone ID 3445301). DDIT3 (clone ID 3530545) and ATF2 (clone ID 240146368) plasmids were also obtained from Open Biosystems and cloned into the eukaryotic expression vector pcDNA3.1. The NRF2 plasmid was obtained from Addgene (plasmid 21459) and has been described previously (23).

The antibodies used in this study were purchased from Santa Cruz Biotechnology: ATF4 (catalog no. sc-200X), CHOP (catalog no. sc-575X), ATF3 (catalog no. sc-188X), CEBPβ (catalog no. sc-150X), MAFF (catalog no. sc-22831X), and CREB1 (catalog no. sc-186). TRIB3 (catalog no. TA303408) and CEBPG (catalog no. TA590102) antibodies were purchased from OriGene. CREB1 (catalog no. 9197) and anti-rabbit (catalog no. 7074S) antibodies were purchased from Cell Signaling Technology.

Luciferase Assay—HEK293 cells seeded in 24-well dishes were cotransfected with 0.3 μg of promoter construct and 1/20× transfected CMV-*Renilla*-expressing plasmid pRLTK (Promega). U2OS cells were seeded in 24-well dishes and cotransfected with 0.75 μg of promoter construct and 1/10× CMV-*Renilla* plasmid. The Dual-Luciferase kit (Promega) was used to measure luciferase and *Renilla* luminescence according to the protocol of the manufacturer protocol with a LB941 TriStar luminometer (Berthold). Firefly luciferase data were normalized to the cotransfected CMV-*Renilla* luminescence (luciferase/*Renilla*). Normalized luciferase values are expressed relative to untreated cells of the longest promoter, set equal to one. Each experiment was performed at least twice, with three biological samples per treatment.

IM-EMSA—HEK293 cells were grown in 100-mm dishes and harvested in 1 ml of lysis buffer (10 mM Hepes (pH 8), 1.5 mM $MgCl_2$, 10 mM KCl, 1 mM DTT, 1% Igepal-CA630, and protease inhibitors (Sigma, catalog no. P8340)). Nuclei were pelleted, and the nuclear extracts were collected using 20 mM Hepes (pH 8), 1.5 mM $MgCl_2$, 25% glycerol, 420 mM NaCl, 0.4 mM EDTA, 1 mM DTT, and protease inhibitors. Nuclear extracts were incubated at 4 °C for 30 min in binding buffer (20 mM Hepes (pH 8),

50 mM KCl, 0.1 mM EDTA, 1 mM $MgCl_2$, 0.1 mg/ml poly-dIdC, and 0.1% Nonidet P-40) with selected unlabeled oligonucleotides. Then the samples were resolved on 6% DNA retardation gels (Invitrogen, catalog no. EC6365) in 0.5× Tris borate-EDTA running buffer (Invitrogen) and transferred to a Hybond N+ membrane (GE Life Sciences, catalog no. RPM203B) in 0.5× Tris borate-EDTA buffer at 4 °C. Next the membranes were dried, UV-cross-linked, and blocked for 30 min in 5% milk/1× TBS-T (Tris-buffered saline and Tween 20). The blots were incubated in blocking buffer containing the indicated antibodies for 1 h, washed three times in TBS-T, and then incubated with secondary antibody diluted in blocking buffer. The blots were washed and developed using ECL-prime and ECL-film (GE Life Sciences).

Immunoblotting—Immunoblots were performed as described previously (14) with the following modifications. 5% skim milk/TBS-T was used for blocking, and primary antibodies were incubated overnight at 4 °C with shaking.

ChIP—ChIP assays were performed as described previously (24) with the following minor modifications. HEK293 cells were seeded in 100-mm dishes with DMEM supplemented with 10% FBS and 1% penicillin-streptomycin and grown to 90% confluence at 37 °C. ER stress was induced by 3 μM thapsigargin treatment for 4 h. After treatment, the cells were pelleted and resuspended in 1 ml of PBS containing protease inhibitors (Sigma). Formaldehyde was added (1% final concentration) to cross-link chromatin and quenched 10 min later by the addition of glycine (0.125 M final concentration). Cross-linked chromatin was sheared for 10 bursts of 20 s/sample, spaced by 4-min cooling in an ice-ethanol bath. Extracts were incubated with 2–5 μg/ml ATF4 antibody or 2 μg/ml ATF3 or CEBPβ antibody overnight at 4 °C with shaking. Chromatin-antibody complexes were captured by incubation with protein A-agarose beads (Millipore, catalog no. 16-157). The DNA fragments were released by incubation with NaCl (0.2 M final concentration) overnight at 65 °C. The fractions were treated with Proteinase K (0.1 mg/ml final concentration), and the DNA was purified using a QIAquick PCR purification kit (Qiagen). Two or more independent ChIP experiments were performed, and at least four independent samples were analyzed for each treatment. No antibody samples were used as negative controls and showed little or no binding. Validation of the ChIP was performed with primers specific to JMJD3, shown previously to contain ATF4 and ATF3 (R1) enrichment or no enrichment (R5) (25). Only samples with >2-fold enrichment at R1 compared with R5 passed the validation.

Real-time PCR Analysis—DNA enrichment was determined using quantitative real-time PCR with a LightCycler 480 II machine and LightCycler 480 SYBR Green I Master Mix (Roche) using the following primers: −3 kb forward, GCCAGGAGCAAGATCAGGTT; −3 kb reverse, CTCCCACCCTGACCAAAGTC; −1 kb forward, CACTTCCCGGACTACAACCC; −1 kb reverse, TGAGCACCTCCTTTGTTGGT; 0 kb forward, TGGAGCTGAACCAATCAGCG; 0 kb reverse, GTGGGGCAAATCCCCTTTTG; +1 kb forward, CCACCTTCCCCTGCATGAAT; +1 kb reverse, TTATCAATCCCGCTGACCCG; +3 kb forward, GTCTCCAAGAGCCTCGATCC; and +3 kb reverse, AGGTGGAATTCCCAGGGCTA. Cycle conditions were as follows: 95 °C for 5 min, followed by 50 cycles of 95 °C for 10 s, 60 °C for 10 s, and 72 °C for 10 s. All data used were within the linear range of detection as determined using the pooled standard curve method. Relative enrichments are reported as the amount of immunoprecipitated DNA (bound fraction) divided by the input DNA (input fraction, 10% of total DNA) and expressed as the bound/input ratio.

Glutathione Assay—After treatment, cells were rinsed with 1× PBS and lysed in 50 μl of 10 μM diethylenetriamine pentaacetate, 0.1% Triton X-100, and 1× PBS. Glutathione was measured using the Tietze recycling assay (26) as described previously. Glutathione concentrations were normalized to total protein concentration as measured by protein assay (Bio-Rad) according to the protocol of the manufacturer.

Statistical Analysis—All reported values are mean ± S.E.M. Two-way analysis of variance with Bonferroni post test was used unless noted otherwise. Significance was accepted when $p < 0.05$.

Results

Bioinformatic Analysis of the Human CHAC1 Promoter Identifies the ATF/CRE, ACM, and CARE Sites—The online bioinformatic tool TFSEARCH was used to analyze the putative promoter sequence upstream of the human *CHAC1* gene for transcription factor binding predictions on the basis of known DNA binding consensus sequences. A highly conserved ATF/CRE consensus sequence at −267 was identified (CTGACGCAAT) along with a −209 CARE sequence (GTTGCATCAC) on the negative strand, which is consistent with the mouse Atf4 consensus sequence as determined by ChIP sequencing (27) (Fig. 1*A*). In addition, a highly conserved element at −248 (CCTTGCTGCA) was identified that did not fit a known transcription factor binding site consensus sequence. We termed the element at −248 the ACM. Also noted were two CCAAT elements, one on the positive strand at −107 and one on the negative strand at −167, and basal −80 CCAAT and −23 TATA boxes. All identified transcription binding factor sequences were highly conserved from *Xenopus tropicalis* to *Homo sapiens,* suggesting that the transcriptional regulation of *CHAC1* has been tightly constrained (Fig. 1*A*).

We noted a discrepancy in the annotation of the translation start on the basis of information from the GENECODE v19 dataset. The ATG codon in the context "MGGAQL . . . " is listed on the University of California Santa Cruz (UCSC) database as the start codon of the human CHAC1 gene. Although the CHAC1 protein sequence is highly conserved in vertebrates, the first ATG (MGGAQL . . .) is not present in murine, canine, elephant, or chicken homologs. Conversely, a downstream, in-frame ATG-codon in the context "MKQESA" is well conserved in these species and is annotated as the start codon for these species in the UCSC database, suggesting that this downstream ATG represents the start codon of human CHAC1 as well. An explanation for the annotation of MGGAQL as the translation start for the CHAC1 gene is its presence in-frame with the conserved CHAC1 sequence.

To determine the correct codon for translation, the *CHAC1* promoter was cloned upstream of a promoterless luciferase construct with (+ATG) and without (−ATG) the proposed ATG

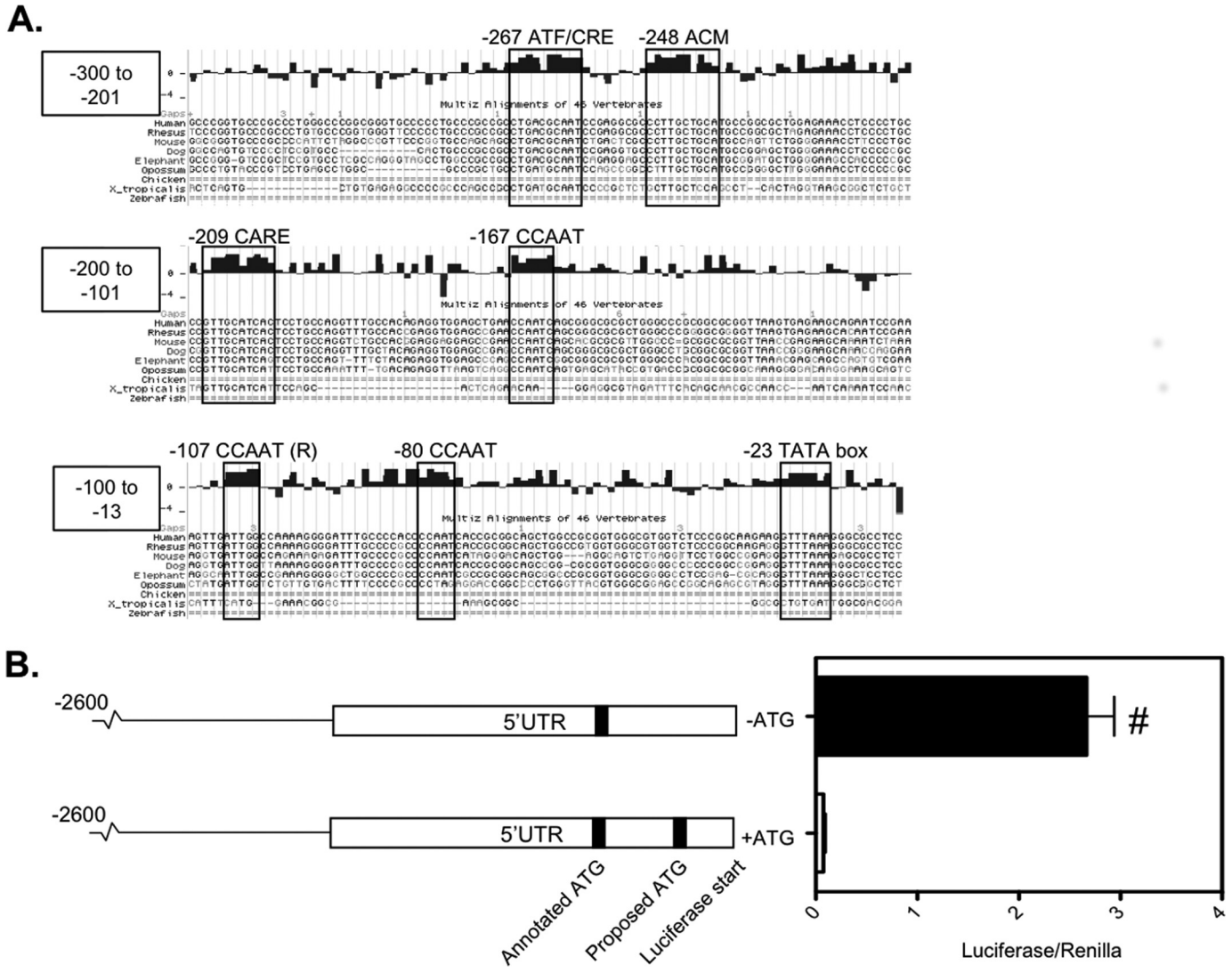

FIGURE 1. **Bioinformatic identification of *CHAC1* promoter elements and the translation start site.** *A*, using an online bioinformatics tool, the CHAC1 promoter sequence was probed for known transcription factor binding motifs. Those discovered are highlighted by *boxes* and overlaid onto the multiZ alignment of this locus available from the UCSC genome browser. *CCAAT (R)* refers to a CCAAT box found on the reverse strand. *B*, luciferase constructs containing 2.6 kb upstream of the *CHAC1* transcriptional start and 133 bp of the 5′UTR (including the annotated translation start site) with (+ATG) or without (−ATG) the proposed CHAC1 start codon were cotransfected with 1/20× CMV-*Renilla*. Raw luciferase values were normalized to raw *Renilla* values (Student's *t* test; #, $p < 0.001$).

(MKQESA). Both constructs contained the upstream, in-frame ATG (MGGAQL) currently annotated as translation start. These constructs were used for the promoter reporter assay scoring firefly luciferase activity normalized to a cotransfected plasmid containing CMV-driven *Renilla* in human HEK293 cells. When the proposed ATG was present (+ATG), minimal luciferase activity was observed (Fig. 1*B*) because the presence of ATG leads to a frameshift in luciferase, disrupting translation. However, removing the proposed ATG (−ATG) led to robust luciferase activity (Fig. 1*B*) as luciferase begins in-frame. These data demonstrate that the proposed ATG (MKQESA) directs the start of translation.

The ATF/CRE and ACM Direct CHAC1 Transcription—To define elements necessary for basal and stress-induced transcription of CHAC1 mRNA, a 2.6-kb region upstream of the transcription start site and the 5′UTR (133 bp) from the human *CHAC1* gene, excluding the ATG defined as translation start in Fig. 1*B*, was cloned upstream of a promoterless firefly luciferase reporter construct (−2600/+133, Fig. 2). This construct and its derivatives were used for promoter reporter assays scoring firefly luciferase activity normalized to a cotransfected plasmid containing CMV-driven *Renilla* in human HEK293 cells. We assayed basal promoter activity and activity following ER stress induced by tunicamycin or thapsigargin (1). Basal transcription of human *CHAC1* was primarily defined by a region between −267 to +133 relative to transcription start (Fig. 2) because further deletion of the upstream region of human CHAC1 resulted in minimal induction under basal as well as ER stress conditions. A 4.5-fold induction of activity after tunicamycin treatment and a 7- to 10-fold induction of activity after thapsigargin treatment were observed when this region was present. Interestingly, 2.5-fold promoter induction was also seen using the amino acid starvation stimulus histidinol, suggesting that CHAC1 is induced by a

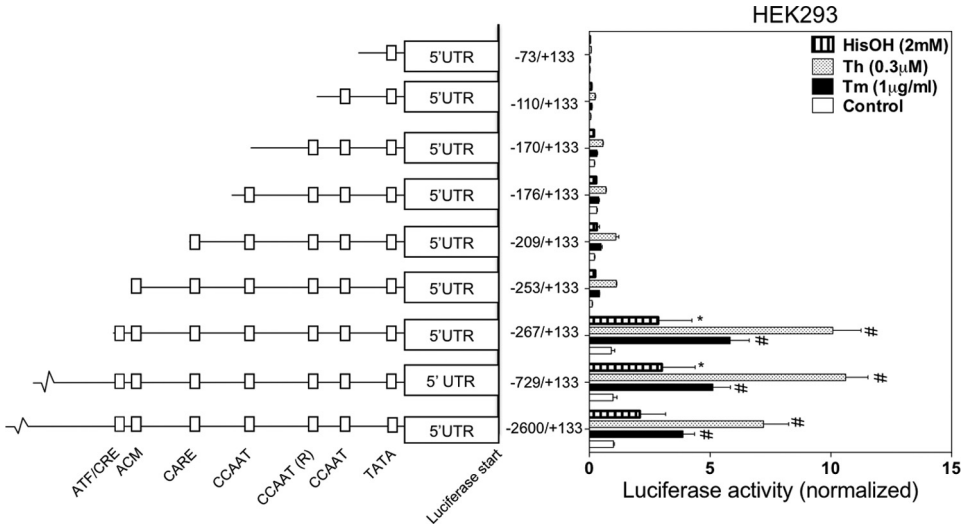

FIGURE 2. **Robust ER stress induction of the human *CHAC1* promoter requires the ATF/CRE in HEK293 cells.** The sequence containing 2.6 kb upstream of the *CHAC1* transcriptional start and 133 bp of the 5′UTR without the *CHAC1* ATG start codon was cloned upstream of a luciferase reporter gene. Each construct was cotransfected with 1/20× CMV-*Renilla*. Raw luciferase values were normalized to raw *Renilla* values and then to −2600/+133 treated with control media, which was set equal to one. The locations of predicted regulatory sites are shown with *open boxes*. Treatments were thapsigargin (Th), tunicamycin (Tm), and histidinol (HisOH) for 24 h. *, $p < 0.05$; #, $p < 0.001$.

broad range of stimuli as part of the integrated stress response rather than just ER stress.

Because the ER stress transcription factor ATF4 plays a role in bone formation (10), we examined the regulation of the CHAC1 promoter in the human osteosarcoma cell line U2OS. (Fig. 3). Thapsigargin treatment led to a 20-fold increase in activity, tunicamycin treatment led to a 5-fold increase in activity, and histidinol treatment led to a 10-fold increase in activity. These data reveal a more robust response of the CHAC1 promoter to histidinol in U2OS cells compared with HEK293, suggesting a role for CHAC1 as an ATF4 target gene functioning in the osteoblast, promoting osteoblast differentiation and function.

Notably, deletion of the ATF/CRE site led to a significant (~90%) decrease in luciferase activity and abrogation of the ER stress response, indicating that the ATF/CRE site is the major site of *CHAC1* transcriptional regulation in both HEK293 and U2OS cells (−253/+133, Figs. 2 and 3). These data highlight a critical role for the ATF/CRE site in the regulation of human *CHAC1* transcription. This result was surprising because the CARE site in the mouse *Chac1* promoter regulates the response to 24-h tunicamycin treatment and ATF4 coexpression (28). Additionally, the CARE site matches the ATF4 DNA binding motif (27), regulates many other ATF4-responsive genes (29), and is highly conserved. Therefore, we further explored the relative contributions of the ATF/CRE, ACM, and CARE sites to *CHAC1* promoter-directed transcriptional activity.

To investigate the independent contributions of the proposed regulatory sites to *CHAC1* promoter-directed transcriptional activity, the ATF/CRE, ACM, and CARE sequences were mutated by directed mutagenesis to scramble the entire site or create stepwise, two-nucleotide mutations (Fig. 4). Mutants were made using a cloning site that was added to the −267/+133 plasmid, which did not change basal or induced activity (data not shown). Scrambled mutations and two-nucleotide mutations in the ATF/CRE site reduced basal activity by 70–75% in HEK cells (Fig. 4*A*) and 90% in U2OS cells (Fig. 5*A*). In HEK cells, the induction of *CHAC1* in response to tunicamycin treatment was abolished in all mutants (Fig. 4*A*). Thapsigargin treatment still led to induced transcriptional activity from the *CHAC1* promoter, although this was much lower compared with the wild-type promoter (Fig. 4*A*). In U2OS cells, the response to either tunicamycin or thapsigargin treatment was abolished following scrambled or stepwise mutations (Fig. 5*A*). These data confirm that the ATF/CRE site plays a major role in the regulation of *CHAC1* transcription and suggest that small contributions from other sites can direct ER stress-induced transcriptional activity if the ATF/CRE site is unavailable.

In HEK293 cells, scrambling the ACM element led to a 60% decrease in basal activity and similar decreases following treatment with ER stress agonists (Fig. 4*B*). Double nucleotide mutations in the second half of this element (ACM mut2 and ACM mut3) led to 50% reductions in activity, whereas the ACM mut1 maintained induction similar to the wild type (Fig. 4*B*). ACM mut2 appeared to be slightly induced by tunicamycin, although this change was not statistically significant. However, the response to thapsigargin remained in the ACM mutants. In U2OS cells, scrambling or stepwise mutations in the ACM abolished the response of the promoter to tunicamycin. The response to thapsigargin remained in every mutant, although the activity was decreased in the scrambled mutant and ACM mut2 (Fig. 5*B*). These data suggest that the middle of the ACM contains the core sequence for transcription factor binding because ACM mut2 induction was most disrupted and define a corollary role for the ACM element in the regulation of the human *CHAC1* promoter.

Interestingly, scrambling or stepwise mutations of the CARE site of the human *CHAC1* promoter resulted in little change in activity (~15%) compared with the wild type in HEK293 cells (Fig. 4*C*). In U2OS cells, there is a loss of tunicamycin induction when the CARE site is mutated, although this is likely because

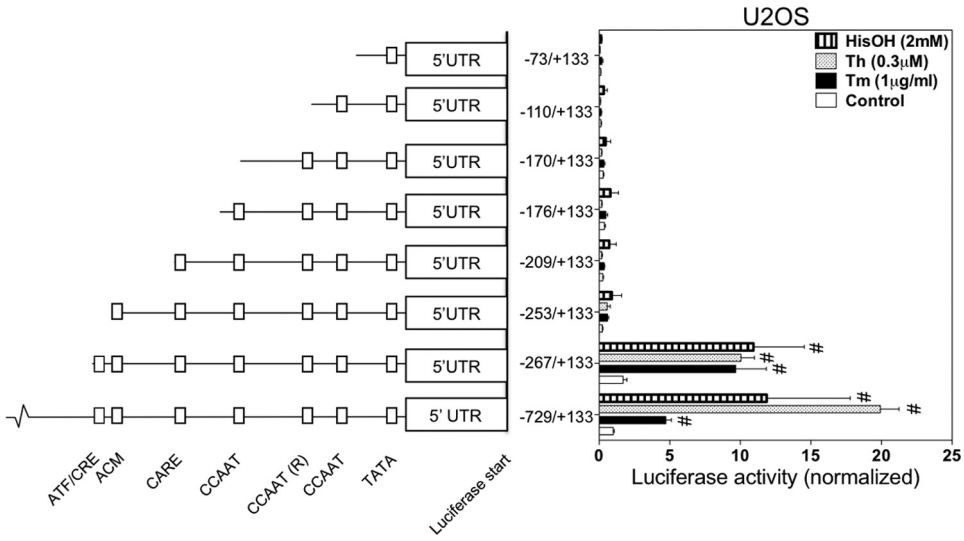

FIGURE 3. **Robust ER stress induction of the human *CHAC1* promoter requires the ATF/CRE in U2OS cells.** Each construct was cotransfected with 1/20× CMV-*Renilla*. Raw luciferase values were normalized to raw *Renilla* values and then to −2600/+133 treated with control media, which was set equal to one. The locations of predicted regulatory sites are shown with *open boxes*. Treatments were Th, Tm, and HisOH for 24 h. *, $p < 0.05$; #, $p < 0.001$.

of the relatively low induction in these cells compared with the robust response in HEK293 cells (Fig. 5*C*). These data provide further support for the hypothesis that the CARE is not critical for transcriptional activity of the human *CHAC1* promoter for basal transcription or ER stress induction and highlight differences in *CHAC1* promoter regulation in the human and mouse.

Because the ATF/CRE and ACM elements appear to direct human *CHAC1* transcriptional activity, we explored the ability of these elements to drive transcription in the absence of other promoter sequences by creating internal deletions within the promoter constructs. Following deletion of all elements except the ATF/CRE, ACM, and TATA box, 50% activity from the luciferase reporter was observed in both HEK293 and U2OS cells (*Del −234/−73*; Fig. 6, *A* and *B*). These data further support a central role for the ATF/CRE and ACM sites in directing transcription of the human *CHAC1* promoter, whereas the CARE site and other intervening sequences have minor roles.

ATF4 and CEBPβ Increase CHAC1 Promoter Activity—To investigate which transcription factors direct *CHAC1* promoter activity, expression plasmids containing several transcription factors were cotransfected with luciferase reporter plasmids in HEK293 cells. The expression of each transcription factor following transfection was verified by immunoblotting (Fig. 7*B*) or GFP fluorescence (NRF2). ATF4 cotransfection led to a 10-fold increase in luciferase activity from the *CHAC1* promoter, similar to previous reports (30). This increase in activity was reduced after the ATF/CRE site was scrambled (Fig. 7*A*). Slight decreases in luciferase activity were also observed after mutation of the ACM or CARE sites. However, these were not as dramatic as ATF/CRE mutation (Fig. 7*A*). These results support a role for ATF4 regulation of *CHAC1* transcription at the ATF/CRE site, with minor contributions from the ACM and CARE site.

ATF4 activity is regulated by *CEBPβ*, which encodes three different transcription factors because of translation from multiple reading frames: LAP*, LAP, and LIP. Each isoform has differential downstream targets and effects. To define the effects of these three forms, LAP only, LIP only, and full-length plasmids were investigated. Full-length CEBPβ led to a 7-fold increase in transcriptional activity from the *CHAC1* promoter (Fig. 7*A*), which was decreased modestly by mutation in any of the three regulatory sites defined previously (Fig. 7*A*). LAP cotransfection increased transcriptional activity 2-fold in wild-type promoters (Fig. 7*A*). This activity was lost following mutation of any of the three sites (Fig. 7*A*). Finally, cotransfection with LIP only did not change transcriptional activity from the *CHAC1* promoter (Fig. 7*A*). Together, these data demonstrate that CEBPβ regulates *CHAC1* expression. Furthermore, LAP* is likely the major CEBPβ isoform, and this effect is not mediated by the ATF/CRE, ACM, or CARE. A minor increase in transcription was also observed in NRF2 and CEBPG cotransfections (Fig. 7*A*). This increase was abolished by mutation of any of the three sites (Fig. 7*A*), suggesting that these transcription factors may make minor contributions in the absence of ATF4. No significant increases in *CHAC1* promoter activity were observed following transfections with other well characterized transcription factors involved in ER stress signaling: MAFF, TRIB3, or CREB1 (Fig. 7*A*).

The CHAC1-ATF4 relationship was predicted from a systems screen of an *in vitro* atherosclerosis model (30). The coexpression coefficient between CHAC1 and ATF4 was higher than known ATF4 target genes, suggesting a more a robust relationship. We investigated the sensitivity of the *CHAC1* promoter response to ATF4 concentration compared with other well characterized ATF4 transcriptional targets, *CHOP* and *ASNS* (31, 32), to determine whether the *CHAC1* promoter is more sensitive to ATF4 regulation. Promoter reporter constructs demonstrating full activity derived from *CHAC1*, *CHOP*, and *ASNS* were cotransfected with varying concentrations of ATF4. Total DNA transfected was kept constant with a GFP expression control plasmid. At the highest ATF4 concentration tested (1×), the *CHOP* promoter was induced 4-fold, the *ASNS* promoter was induced 5-fold, and the *CHAC1* pro-

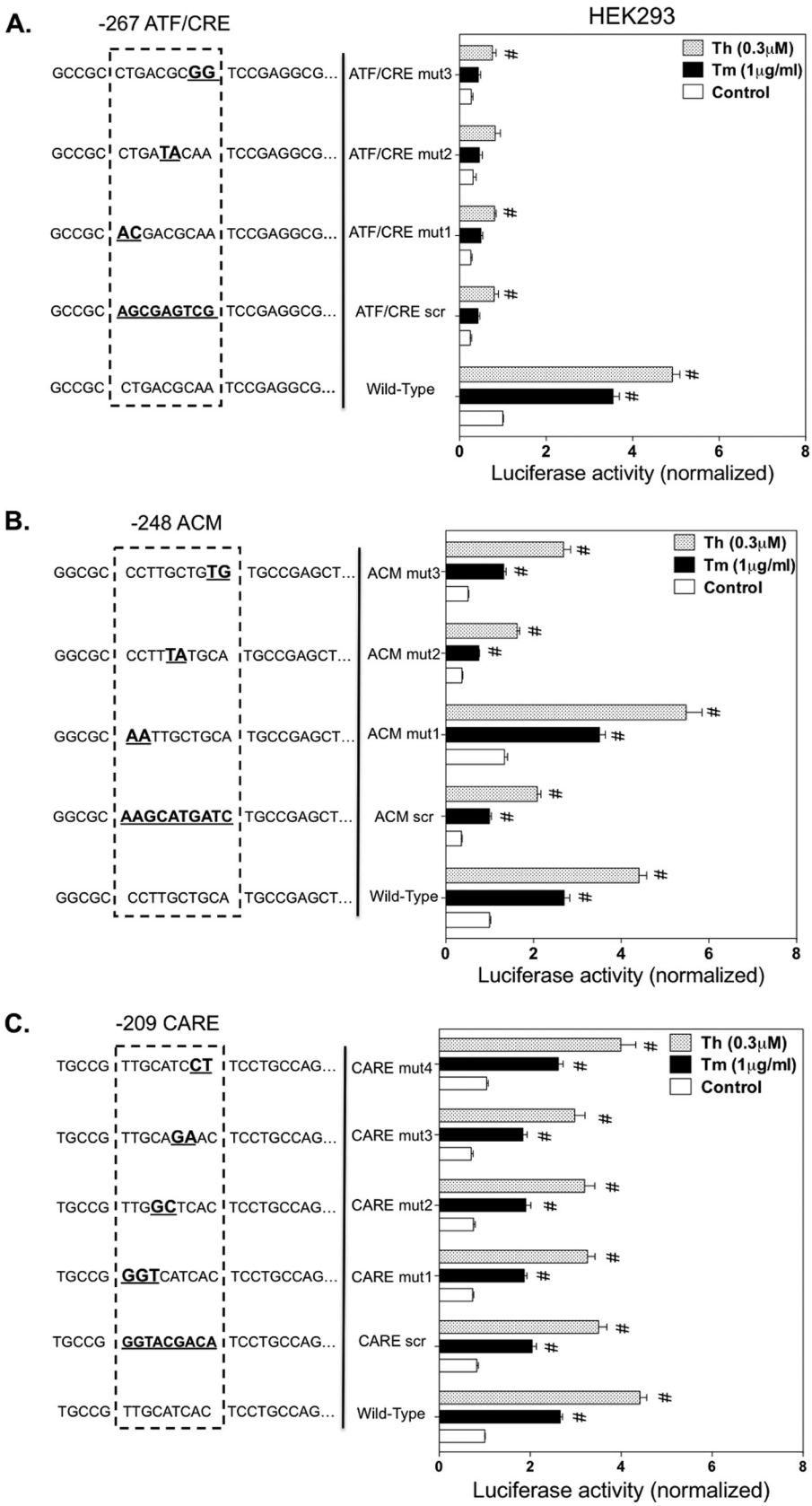

FIGURE 4. **The ATF/CRE and ACM direct transcription of the human *CHAC1* promoter in HEK293 cells.** *A–C*, mutational analysis of the ATF/CRE (*A*), ACM (*B*), and CARE (*C*). Each construct was cotransfected with 1/20× CMV-Renilla. Raw luciferase values were normalized to raw *Renilla* values and then to the wild-type plasmid treated with control. Mutated residues are identified in *boldface* and *underlined*. Treatments were Th and Tm for 24 h. *Scr*, scrambled. *, $p < 0.05$; #, $p < 0.001$.

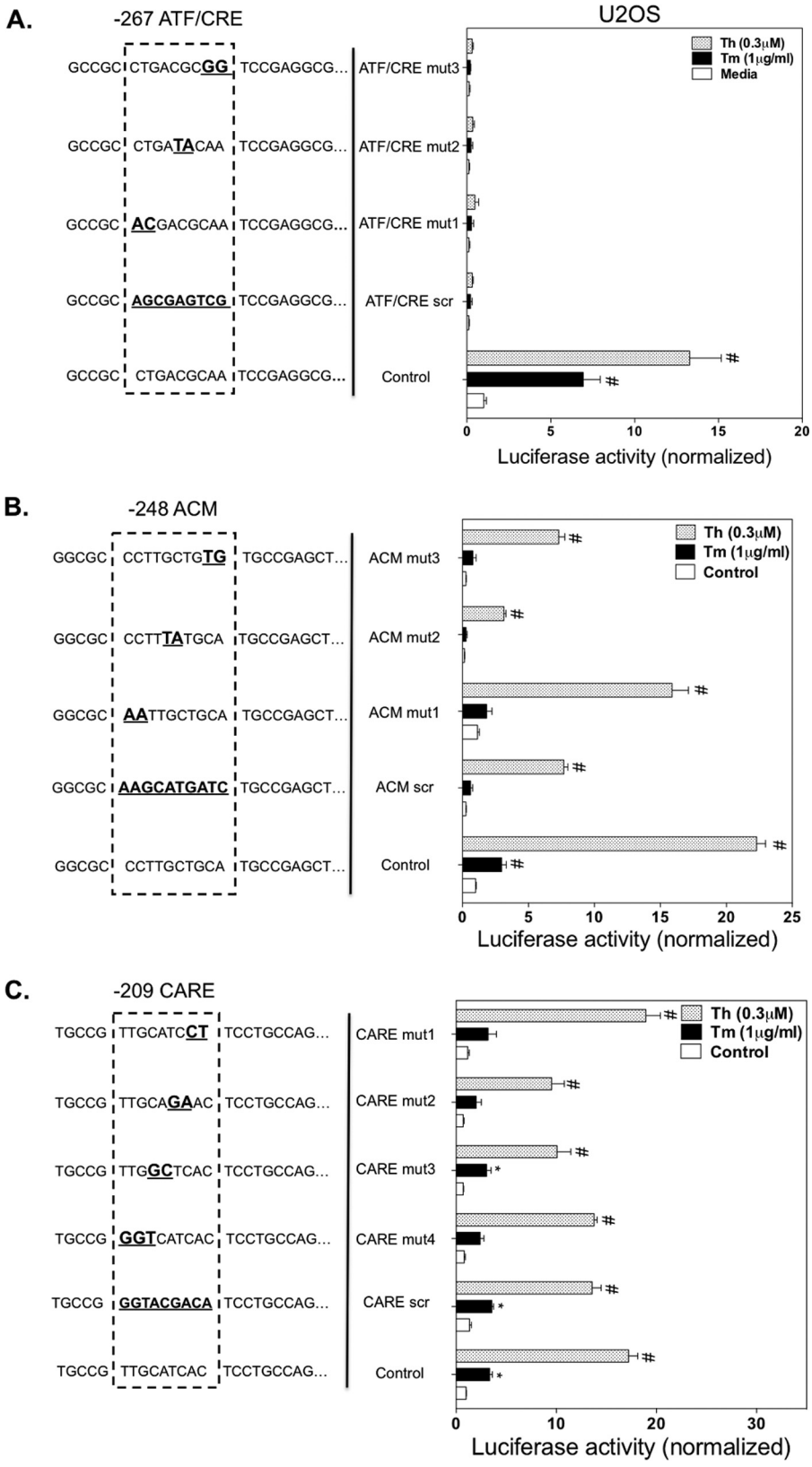

FIGURE 5. **The ATF/CRE and ACM direct transcription of the human *CHAC1* promoter in HEK293 cells.** *A–C*, mutational analysis of the ATF/CRE (*A*), ACM (*B*), and CARE (*C*). Each construct was cotransfected with 1/20× CMV-Renilla. Raw luciferase values were normalized to raw *Renilla* values and then to the wild-type plasmid treated with control. Mutated residues are identified in *boldface* and *underlined*. Treatments were Th and Tm for 24 h. *Scr*, scrambled. *, $p < 0.05$; #, $p < 0.001$.

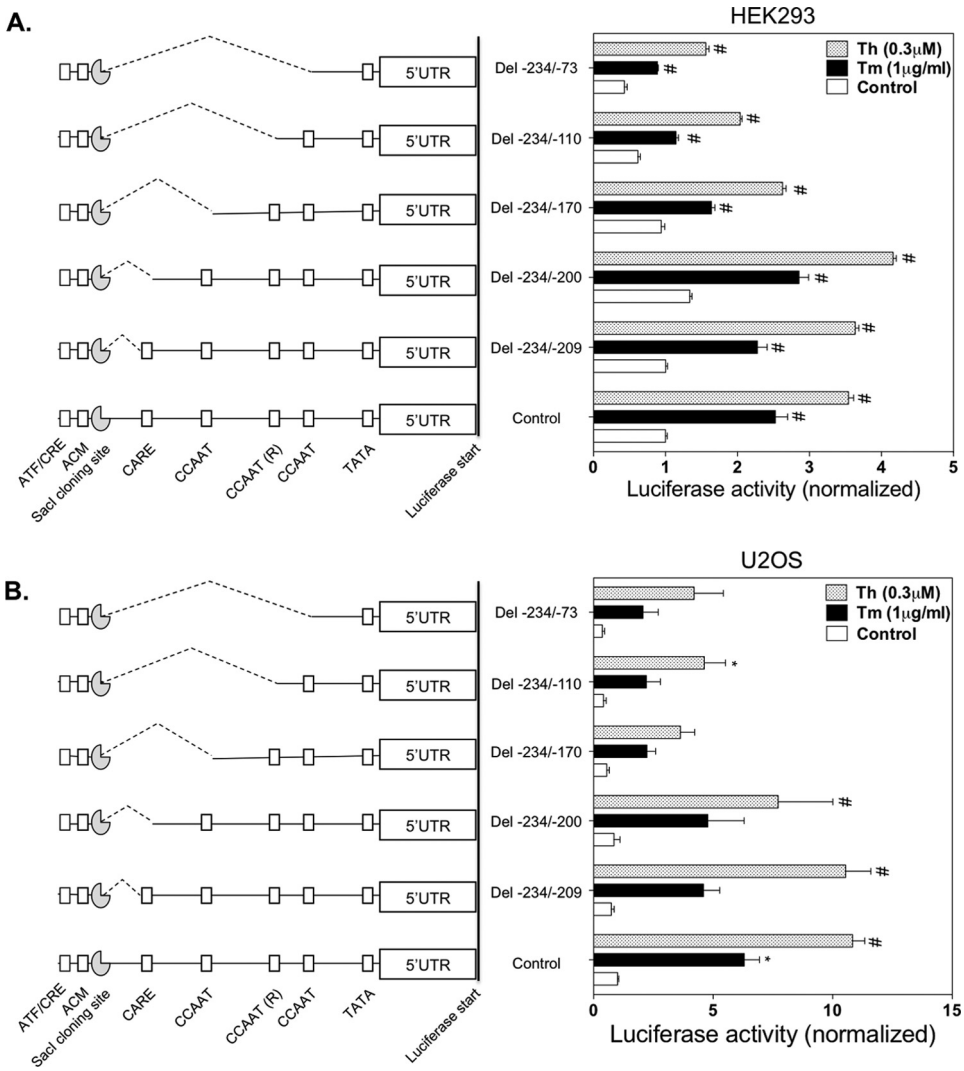

FIGURE 6. **The ATF/CRE and ACM sites drive robust transcription in the absence of other regulatory sequences.** *A* and *B*, internal deletions in the *CHAC1* promoter were created using a Sac1 cloning site. *Dashed lines* encompass the deleted regions. Each construct was cotransfected with 1/20× CMV-*Renilla* in HEK cells (*A*) or U2OS cells (*B*). Raw luciferase values were normalized to raw *Renilla* values and then to the wild-type plasmid. Treatments were Th and Tm for 24 h. *, $p < 0.05$; #, $p < 0.001$.

moter was induced 10-fold (Fig. 8). *CHAC1* promoter induction was also increased above *CHOP* and *ASNS* promoter induction at 1/2× ATF4 concentration. These data suggest that the *CHAC1* promoter reporter constructs are more responsive to ATF4 cotransfection compared with *CHOP* or *ASNS* luciferase reporters.

ATF4 Binds to the ATF/CRE and ACM—To determine the ability of ATF4 and CEBPβ to bind the ATF/CRE and ACM sequences in the human *CHAC1* promoter, we developed the novel IM-EMSA assay. Nuclear extracts were prepared from control or thapsigargin-treated (3 μM, 4 h) HEK293 cells. These nuclear extracts were incubated in oligonucleotide binding buffer with double-stranded oligonucleotides encompassing the human *CHAC1* ATF/CRE, ACM, or scrambled versions of these sequences (Fig. 9*A*). These binding reactions were separated on a native gel and transferred to a positively charged nylon membrane, where the mobility of several transcription factors was quantified using Western detection with a specific antibody.

The use of IM-EMSA with antibodies directed to candidate target genes is similar to traditional EMSAs. However, instead of monitoring a change in mobility of labeled oligonucleotides, IM-EMSA detects changes in protein mobility using specific antibody detection. Notably, the mobility of free protein was always very slow and migrated at the top of the blot, whereas, in the presence of protein-oligonucleotide complexes, an increase in mobility was observed. This pattern is consistent with the native (non-denaturing) conditions of the assay where proteins migrate on the basis of their net charge in Tris borate-EDTA buffer (pH 8.3). Upon protein binding to DNA, there is a dramatic change in mass-charge, leading to an increased gel migration rate. The net charge of a 30-nucleotide oligonucleotide is −60 compared with the net charge at pH 8.3 calculated for human ATF4 (−23) or ATF3 (+1.1). This novel IM-EMSA approach represents a new tool to rapidly assay protein-DNA binding *in vitro*.

Consistent with previous data, an increase in ATF4 expression accompanied thapsigargin treatment (*none*, Fig. 9*B*).

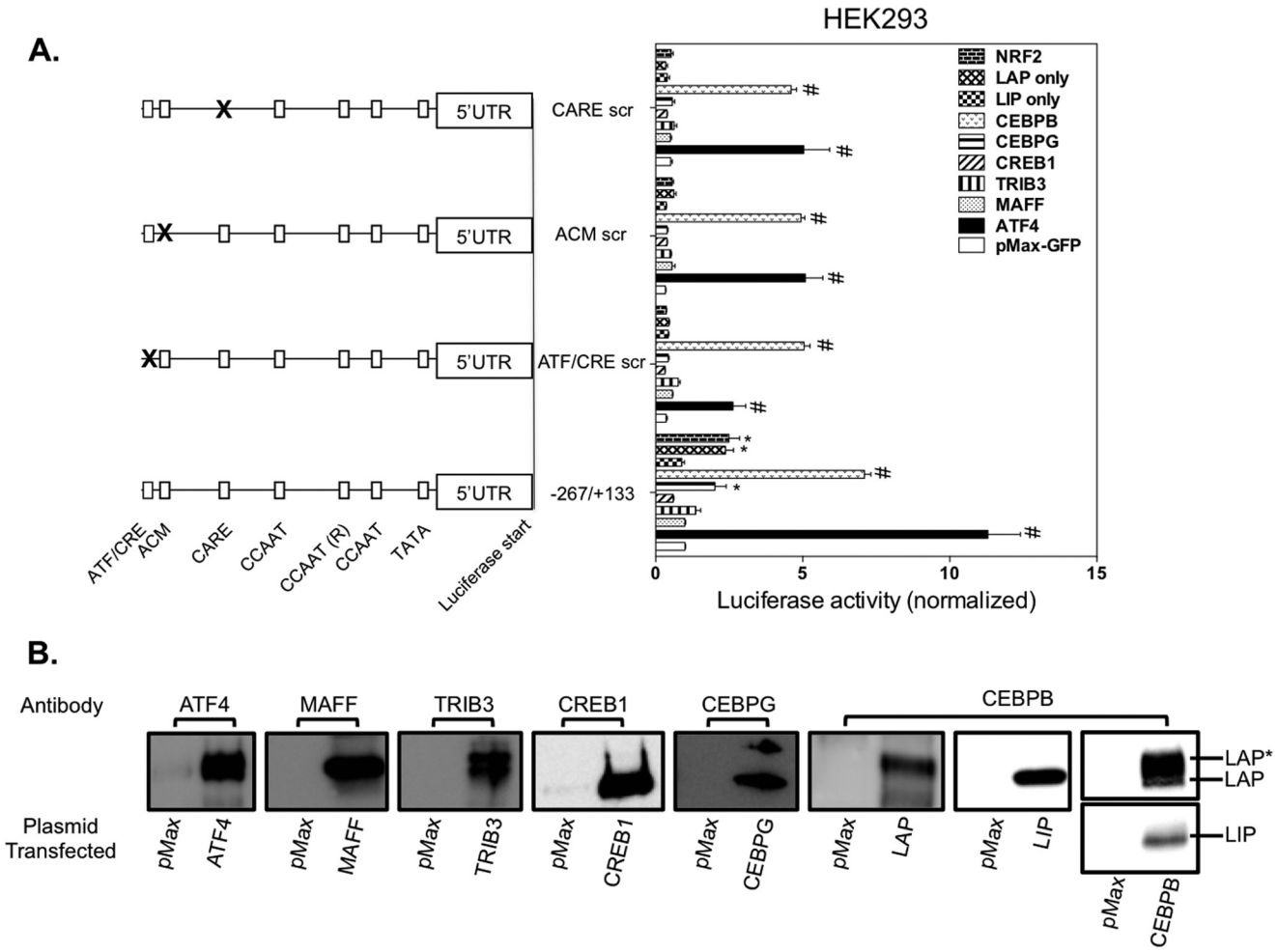

FIGURE 7. **ATF4 and CEBPβ transfection activates the *CHAC1* promoter.** *A*, cotransfection of *CHAC1* promoter reporter plasmids with expression plasmids containing the control plasmid (*pMAX-GFP*) or various transcription factors and 1/20× CMV-*Renilla*. Raw luciferase values were normalized to raw *Renilla* values and then to −267/+133 treated with the control. *, $p < 0.05$; #, $p < 0.001$. Mutated sequences are shown with an *X*. *scr*, scrambled. *B*, transcription factor expression was verified using immunoblotting. NRF2 expression was verified using GFP fluorescence prior to harvesting the cells.

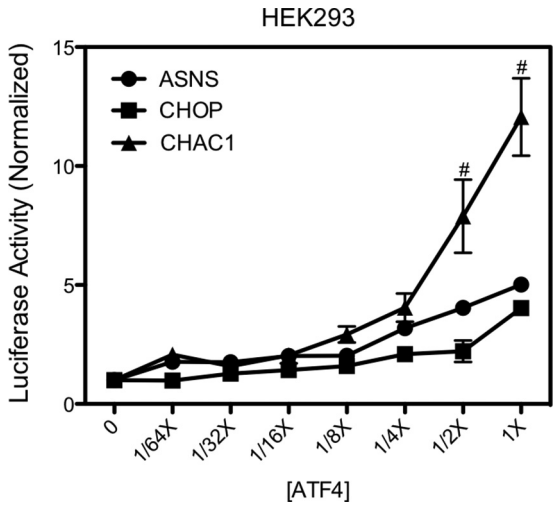

FIGURE 8. **The *CHAC1* promoter luciferase reporter is more responsive to ATF4 than the *CHOP* and *ASNS* promoters.** Luciferase reporter plasmids driven by *CHAC1*, *CHOP*, and *ASNS* promoters with all of the required elements for full activity were cotransfected with varying amounts of ATF4 (1× = 0.15 μg) and 1/20× CMV-*Renilla*. Total DNA was kept constant with a GFP expression plasmid. Raw luciferase values were normalized to raw *Renilla* values and then to the 1× GFP average of each plasmid. #, $p < 0.001$ *versus* ASNS.

When nuclear extracts were incubated in the presence of an ATF/CRE oligonucleotide, a shift in the mobility of ATF4 was observed, consistent with ATF4 binding to the ATF/CRE site (*A*, Fig. 9*B*). A shift was not observed in the presence of a mutant oligonucleotide of the same size (*Mut A*, Fig. 9*B*), suggesting that sequence specificity is required for ATF4 binding at the ATF/CRE site. Incubation with the ACM oligonucleotide also generated a change in ATF4 mobility. However, the intensity of this shifted band was lower, suggesting a weaker interaction. Similarly, mutation of the ACM disrupted ATF4 binding to the ACM, and shifted ATF4 was not observed. These data are consistent with our data suggesting that the ATF/CRE is the major regulatory site in the human *CHAC1* promoter and that the ACM plays a supporting role. Additionally, ATF4 binding to oligonucleotides from previously defined ATF4 CARE sites within the TRIB3 (33) and ATF5 (34) promoters were examined, and specific shifts consistent with binding were noted (data not shown), supporting the use of IM-EMSA to detect ATF4 binding.

To determine what other transcription factors may be binding to the ATF/CRE or ACM, ATF3 and CHOP antibodies were

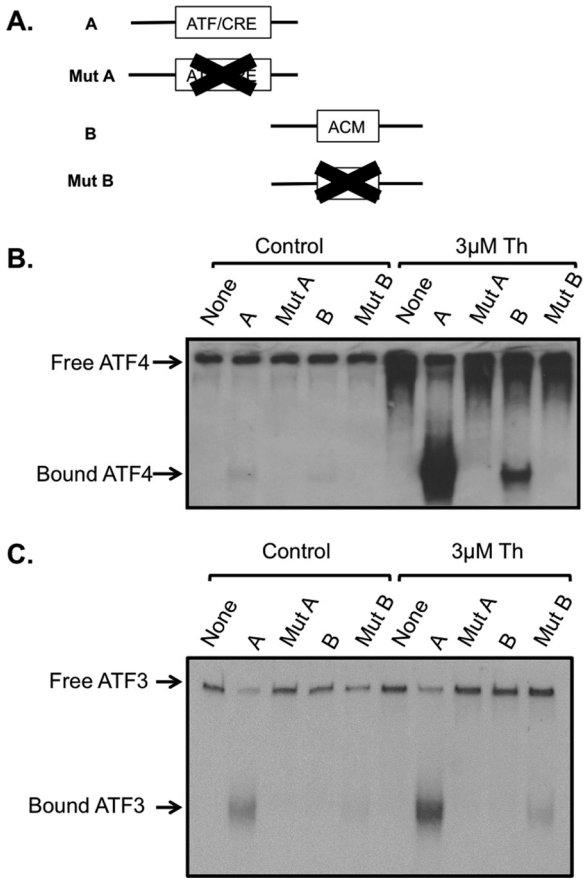

FIGURE 9. **ATF4 binds to both the ATF/CRE and ACM sites, whereas ATF3 binds to the ACM.** *A*, short oligonucleotide probes containing wild-type or mutated ATF/CRE and ACM sequences were incubated with nuclear extract cells treated with 3 μM Th *versus* control for 4 h. *B* and *C*, proteins were separated on a native gels to identify ATF4 (*B*) or ATF3 (*C*) to determine transcription factor binding. Reactions without oligonucleotides (*none*) were included to detect free transcription factors.

used to probe DNA-protein interactions using IM-EMSA. Both ATF3 and CHOP are proteins downstream of ATF4 in the ER stress pathway required for ER stress-induced transcription of CHAC1 mRNA, as measured by quantitative RT-PCR analysis (14). ATF3 binds to the ATF/CRE oligonucleotide at baseline and after treatment but not to the ACM (Fig. 9*C*), suggesting that ATF3 regulates *CHAC1* transcription from the ATF/CRE. No binding at either sequence was observed after probing for CHOP (data not shown), suggesting that CHOP has indirect actions on *CHAC1* transcription.

ATF4, ATF3, and CEBPβ Are Enriched at the CHAC1 Promoter—To confirm ATF4, ATF3, and CEBPβ binding to the human *CHAC1* promoter *in vivo*, which is consistent with data from this and other studies (14, 27, 28, 30), ChIP was performed in HEK293 cells treated with 3 μM thapsigargin for 4 h to induce the ER stress response. We examined enrichment using quantitative PCR with primer sets located near the ATF/CRE and ACM sites (0 kb) or 1 and 3 kb in either direction.

In control cells, ATF4 was not enriched at the *CHAC1* promoter above background (Fig. 10*A*). Induction of ER stress resulted in increased ATF4 protein expression (Fig. 10*D*), as expected, and a significant enrichment of ATF4 near the ATF/CRE site (Fig. 10*A*). These data define enhanced ATF4 binding at the endogenous human *CHAC1* promoter accompanying thapsigargin treatment.

ATF3 enrichment near the ATF/CRE site was observed in control and thapsigargin-treated cells (Fig. 10*B*), which did not accompany an obvious change in ATF3 protein expression (Fig. 10*D*). These data suggest that ATF3 may regulate basal and ER stress-induced *CHAC1* expression.

Similar to ATF4, CEBPβ was not significantly enriched at the *CHAC1* promoter at baseline (Fig. 10*C*), and enrichment near the ATF/CRE site increased following ER stress induction (Fig. 10*C*). We noted a significant increase in the LIP isoform accompanying treatment with thapsigargin and slight decreases in expression of LAP* and LAP that did not reach statistical significance (Fig. 10*D*).These data point to complex possible contributions from various CEBPβ isoforms in the regulation of *CHAC1*. These data define enhanced CEBPβ binding at the endogenous *CHAC1* promoter following thapsigargin treatment.

CHAC1 Depletes Glutathione—Recent reports have shown that mouse and yeast CHAC1 homologs directly degrade glutathione in yeast and cell-free models (15, 16). These reports have also suggested that a conserved glutamate (Glu-115 in humans) is the catalytic residue. To determine the physiological relevance of this activity in a human model, HEK293 cells were transfected with a CHAC1 expression plasmid, and total glutathione was measured using the Tietze assay. Overexpression of CHAC1 led to an 80% reduction in total glutathione (Fig. 11), whereas mutation of the catalytic glutamate to a glutamine (E115Q) abrogated this activity and returned glutathione levels to control levels. These data suggest that human CHAC1 does function to deplete cells of glutathione and requires the conserved catalytic residue Glu-115.

Discussion

We have shown previously that *CHAC1* is functionally linked to *ATF4* using a systems genetics approach (20, 30) and further validated this with knockdown studies (14). Additionally, previous work has illustrated the importance of the ATF/CRE in cell stress and ATF4 action (35, 36). This work validates and expands on previous data, demonstrating ATF4, ATF3, and CEBPβ regulation of the *CHAC1* promoter and providing three lines of evidence implicating two regulatory *cis*-acting elements: the ATF/CRE and ACM.

The ATF/CRE and ACM bipartite element represents a novel ATF4-responsive transcriptional unit. The luciferase reporter assays and selected deletion mutants define the critical requirement for the ATF/CRE for basal and stress-induced transcription. Parallel experiments using ACM mutants demonstrated that this element has a secondary role and potentiates *CHAC1* transcription. A *CHAC1* promoter construct consisting of only the ATF/CRE, ACM, and TATA box led to robust activation that was ~50% of the wild-type construct. The IM-EMSA assay showed interaction of ATF4 with ATF/CRE and ACM in ER stress-induced conditions, and ATF3 binding was seen at the ATF/CRE in basal and stress-induced conditions. ChIP demonstrated ATF4, ATF3, and CEBPβ enrichment in the vicinity of the ATF/CRE and ACM of the *CHAC1* promoter. Collectively, these data

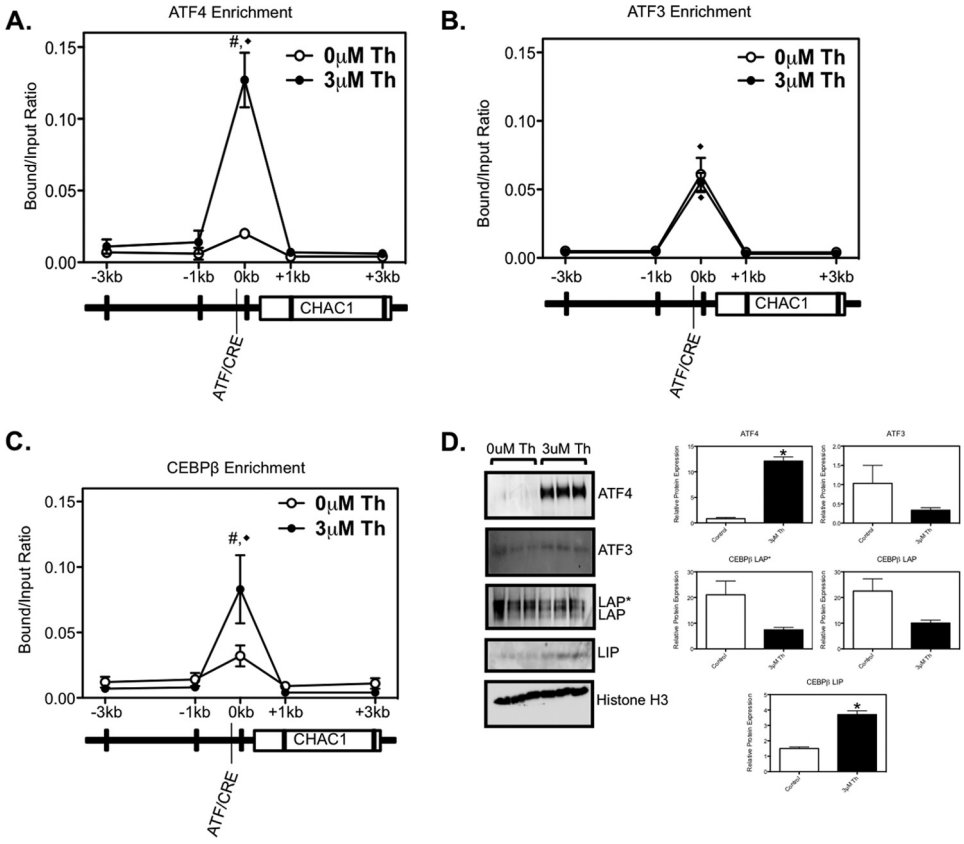

FIGURE 10. **ATF4, ATF3, and CEBPβ are enriched at the *CHAC1* promoter.** HEK293 cells were treated with 0 or 3 μM Th for 4 h. *A*—*C*, ChIP experiments were performed using ATF4 (*A*), ATF3 (*B*), and CEBPβ (*C*) antibodies and primers specific to the region of interest adjacent to the ATF/CRE and ACM (0 kb) or 1 and 3 kb distal. Data are presented as the bound/input ratio. No antibody samples were used as negative controls and showed little or no binding. One-way analysis of variance, Dunnett's post test; #, $p < 0.001$ *versus* 0 μM Th; ♦, $p < 0.05$ *versus* no antibody. *D*, immunoblots and densitometry to determine transcription factor expression. Student's *t* test; *, $p < 0.05$.

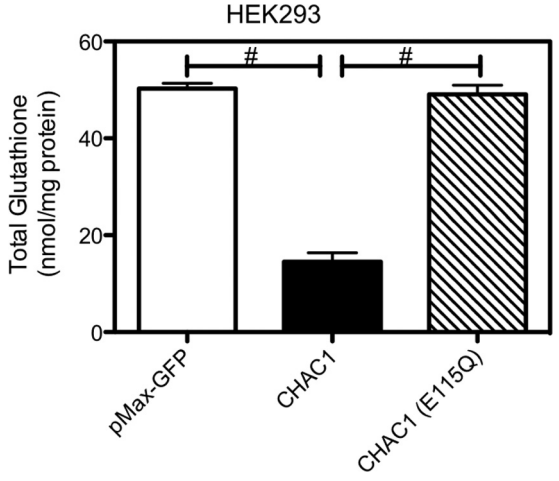

FIGURE 11. **CHAC1 overexpression depletes glutathione.** HEK293 cells were transfected with control (*pMAX-GFP*), CHAC1, or CHAC1-E115Q, a catalytic site mutation, plasmids. Total glutathione was measured by Tietze recycling assay and normalized to total protein. One-way analysis of variance; Bonferroni post test; #, $p < 0.001$.

define a predominant contribution from ATF4 at the ATF/CRE and ACM in the regulation of stress-induced *CHAC1* expression. ATF3 may primarily modulate basal expression through the ATF/CRE. CEBPβ, likely the LAP* isoform, regulates ER stress-induced *CHAC1* expression via an independent site (Fig. 10). Because each of these transcription factors act as dimers, further work is needed to refine the specific protein complexes at each site.

A recent report defined elements responsible for transcriptional activity from the mouse *Chac1* promoter (28). Several differences between the mouse and human promoter are evident. Although the ATF/CRE site appears to be important for *CHAC1* regulation in both species, the CARE site has a more important role in the mouse. Mutation or deletion of the CARE site in the human *CHAC1* promoter led to slight (~15%) decreases in activity at baseline and after ER stress agonist treatment. In contrast, CARE mutations in the mouse *Chac1* promoter dramatically reduced basal activity (>80%) and prevented induction by tunicamycin. The role of the ACM site was not determined in the mouse, but a clear importance for this element was demonstrated in the human promoter in our study. The differences between these reports may reflect species differences with respect to *CHAC1* regulation. Differences could also be a result of the cell types studied in these two reports. The previous report explored *Chac1* induction in Neuro2A cells, a mouse neuronal cell line, whereas we explored *CHAC1* induction in the context of HEK293 cells, a human embryonic epithelial cell line, and U20S, a human osteoblast sarcoma cell line.

Although the *CHAC1* ATF/CRE and ACM are the main positive elements for transcription, it is clear that other elements with regulatory roles exist within the *CHAC1* promoter. For

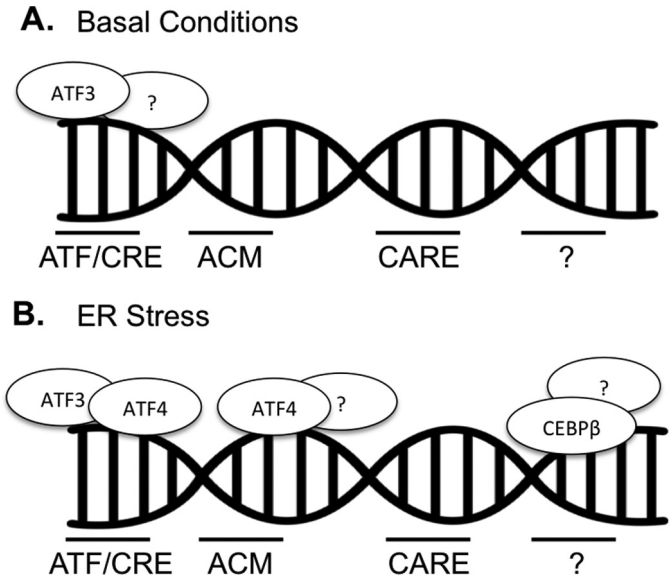

FIGURE 12. **A model for the transcriptional regulation of *CHAC1*.** *A*, under basal conditions, ATF3 with an unknown binding partner regulates *CHAC1* transcription from the ATF/CRE. *B*, induction of the ER stress response leads to ATF4 binding to the ATF/CRE site with ATF3 and to the ACM with an unknown binding partner. CEBPβ is also recruited to the *CHAC1* promoter, increasing transcription.

example, when the area between −2600 and −729 was deleted, an apparent increase in activity was observed (Fig. 2), suggesting that a negative transcriptional regulator may be present in this region. Additionally, the first CCAAT box appears to contribute to regulation because deletion of this region does lead to a slight depression in activity even when the ATF/CRE and ACM sites are present (Fig. 6*A*, *Del −234/−170*). This sequence is a probable candidate for CEBPβ transcription factor binding that will be explored in future studies to refine the role of CEBPβ in the regulation of CHAC1.

The data that explore a role for ATF3 in the regulation of *CHAC1* are paradoxical and suggest complex regulation. We have shown previously that ATF3 knockdown led to the inhibition of ER stress-induced CHAC1 mRNA (14), but the *CHAC1* luciferase reporter is not induced by ATF3 overexpression (30). In this work, we noted significant binding of ATF3 to the *CHAC1* ATF/CRE by IM-EMSA, and ChIP revealed ATF3 enrichment at the *CHAC1* promoter under basal and ER stress conditions. These data suggest a direct effect of ATF3 necessary for regulation of *CHAC1* gene expression, but ATF3 alone is not sufficient for ER stress induction. The data presented here suggest a model in which ATF3 regulates basal transcription through the ATF/CRE site. After ER stress signals facilitate ATF4 maturation, ATF4 is recruited to the ATF/CRE, and CEBPβ is recruited to another site to increase transcription (Fig. 12). What remains unclear is the role of the ACM. It is possible that, under stress conditions, the ACM recruits a separate ATF4-containing complex that further increases CHAC1 transcription cooperatively with the ATF/CRE. Additionally, the spacing of the ATF/CRE and ACM sites is similar to the CARE and NSRE2 motif seen in the *ASNS* promoter (37). We intend to further our study of the ATF/CRE and ACM sequences to define other proteins that regulate CHAC1 expression from these elements. Importantly, the ACM element may be a novel ATF4-responsive target for other genes within the ER stress pathway.

CHAC1 is a proapoptotic (14) enzyme that degrades glutathione in yeast and cell-free systems (15) and promotes neurogenesis through the regulation of Notch (18, 19). Here we demonstrate that CHAC1 overexpression depletes human cells of glutathione. Because of the role of glutathione in cell cycle progression and apoptosis (17), an important role for CHAC1 in regulating the redox potential, proliferation, and viability of cells following ER stress is suggested. CHAC1 induction may induce a biphasic signal, first for cell cycle arrest, allowing the cell time to adapt to the stress, followed by apoptosis if the stress is insurmountable. Future work should elucidate this pathway and may have importance in health and disease because CHAC1 has been implicated in atherosclerosis (30), cancer (38–41), liver metabolism (42), viral infection (43, 44), and retinal axonal damage (45).

ATF4 has been implicated as an initiator of osteoblast differentiation, and *Atf4* knockout mice have defects in bone formation (10). The *Atf4* knockout model also revealed a role for *Atf4* in regulating glucose metabolism because of an effect in the osteoblast (5). Here we validate the expression of *CHAC1* in an osteoblast line, U2OS, and show a robust transcriptional induction by ATF4. These data suggest a role for *CHAC1* as a downstream target of ATF4 that may play important roles in osteogenesis and glucose metabolism.

Acknowledgments—We thank Donna Neumann (Louisiana State University Health Sciences Center) for reagents, methods, and intellectual contributions to the ChIP assay.

References

1. Schröder, M., and Kaufman, R. J. (2005) The mammalian unfolded protein response. *Annu. Rev. Biochem.* **74,** 739–789
2. Tabas, I., and Ron, D. (2011) Integrating the mechanisms of apoptosis induced by endoplasmic reticulum stress. *Nat. Cell Biol.* **13,** 184–190
3. Bernales, S., Papa, F. R., and Walter, P. (2006) Intracellular signaling by the unfolded protein response. *Annu. Rev. Cell Dev. Biol.* **22,** 487–508
4. Harding, H. P., Novoa, I., Zhang, Y., Zeng, H., Wek, R., Schapira, M., and Ron, D. (2000) Regulated translation initiation controls stress-induced gene expression in mammalian cells. *Mol. Cell* **6,** 1099–1108
5. Yoshizawa, T., Hinoi, E., Jung, D. Y., Kajimura, D., Ferron, M., Seo, J., Graff, J. M., Kim, J. K., and Karsenty, G. (2009) The transcription factor ATF4 regulates glucose metabolism in mice through its expression in osteoblasts. *J. Clin. Invest.* **119,** 2807–2817
6. Xiao, G., Zhang, T., Yu, S., Lee, S., Calabuig-Navarro, V., Yamauchi, J., Ringquist, S., and Dong, H. H. (2013) ATF4 protein deficiency protects against high fructose-induced hypertriglyceridemia in mice. *J. Biol. Chem.* **288,** 25350–25361
7. Gargalovic, P. S., Gharavi, N. M., Clark, M. J., Pagnon, J., Yang, W.-P., He, A., Truong, A., Baruch-Oren, T., Berliner, J. A., Kirchgessner, T. G., and Lusis, A. J. (2006) The unfolded protein response is an important regulator of inflammatory genes in endothelial cells. *Arterioscler. Thromb. Vasc. Biol.* **26,** 2490–2496
8. Berisha, S. Z., Hsu, J., Robinet, P., and Smith, J. D. (2013) Transcriptome analysis of genes regulated by cholesterol loading in two strains of mouse macrophages associates lysosome pathway and ER stress response with atherosclerosis susceptibility. *PLoS ONE* **8,** e65003
9. Yang, X., and Karsenty, G. (2004) ATF4, the osteoblast accumulation of which is determined post-translationally, can induce osteoblast-specific gene expression in non-osteoblastic cells. *J. Biol. Chem.* **279,** 47109–47114

10. Yang, X., Matsuda, K., Bialek, P., Jacquot, S., Masuoka, H. C., Schinke, T., Li, L., Brancorsini, S., Sassone-Corsi, P., Townes, T. M., Hanauer, A., and Karsenty, G. (2004) ATF4 is a substrate of RSK2 and an essential regulator of osteoblast biology; implication for Coffin-Lowry syndrome. *Cell* **117,** 387–398
11. Chen, G. K., Sale, S., Tan, T., Ermoian, R. P., and Sikic, B. I. (2004) CCAAT/enhancer-binding protein β (nuclear factor for interleukin 6) transactivates the human MDR1 gene by interaction with an inverted CCAAT box in human cancer cells. *Mol. Pharmacol.* **65,** 906–916
12. Ramji, D. P., and Foka, P. (2002) CCAAT/enhancer-binding proteins: structure, function and regulation. *Biochem. J.* **365,** 561–575
13. Li, Y., Bevilacqua, E., Chiribau, C.-B., Majumder, M., Wang, C., Croniger, C. M., Snider, M. D., Johnson, P. F., and Hatzoglou, M. (2008) Differential control of the CCAAT/enhancer-binding protein β (C/EBPβ) products liver-enriched transcriptional activating protein (LAP) and liver-enriched transcriptional inhibitory protein (LIP) and the regulation of gene expression during the response to endoplasmic reticulum stress. *J. Biol. Chem.* **283,** 22443–22456
14. Mungrue, I. N., Pagnon, J., Kohannim, O., Gargalovic, P. S., and Lusis, A. J. (2009) CHAC1/MGC4504 is a novel proapoptotic component of the unfolded protein response, downstream of the ATF4-ATF3-CHOP cascade. *J. Immunol.* **182,** 466–476
15. Kumar, A., Tikoo, S., Maity, S., Sengupta, S., Sengupta, S., Kaur, A., and Bachhawat, A. K. (2012) Mammalian proapoptotic factor ChaC1 and its homologues function as γ-glutamyl cyclotransferases acting specifically on glutathione. *EMBO Rep.* **13,** 1095–1101
16. Tsunoda, S., Avezov, E., Zyryanova, A., Konno, T., Mendes-Silva, L., Pinho Melo, E., Harding, H. P., and Ron, D. (2014) Intact protein folding in the glutathione-depleted endoplasmic reticulum implicates alternative protein thiol reductants. *eLife* **3,** e03421
17. Aquilano, K., Baldelli, S., and Ciriolo, M. R. (2014) Glutathione: new roles in redox signaling for an old antioxidant. *Front. Pharmacol.* **5,** 196
18. Chi, Z., Zhang, J., Tokunaga, A., Harraz, M. M., Byrne, S. T., Dolinko, A., Xu, J., Blackshaw, S., Gaiano, N., Dawson, T. M., and Dawson, V. L. (2012) Botch promotes neurogenesis by antagonizing Notch. *Dev. Cell* **22,** 707–720
19. Chi, Z., Byrne, S. T., Dolinko, A., Harraz, M. M., Kim, M.-S., Umanah, G., Zhong, J., Chen, R., Zhang, J., Xu, J., Chen, L., Pandey, A., Dawson, T. M., and Dawson, V. L. (2014) Botch is a γ-glutamyl cyclotransferase that deglycinates and antagonizes Notch. *Cell Rep.* **7,** 681–688
20. Romanoski, C. E., Lee, S., Kim, M. J., Ingram-Drake, L., Plaisier, C. L., Yordanova, R., Tilford, C., Guan, B., He, A., Gargalovic, P. S., Kirchgessner, T. G., Berliner, J. A., and Lusis, A. J. (2010) Systems genetics analysis of gene-by-environment interactions in human cells. *Am. J. Hum. Genet.* **86,** 399–410
21. Su, N., and Kilberg, M. S. (2008) C/EBP homology protein (CHOP) interacts with activating transcription factor 4 (ATF4) and negatively regulates the stress-dependent induction of the asparagine synthetase gene. *J. Biol. Chem.* **283,** 35106–35117
22. Gargalovic, P. S., Imura, M., Zhang, B., Gharavi, N. M., Clark, M. J., Pagnon, J., Yang, W.-P., He, A., Truong, A., Patel, S., Nelson, S. F., Horvath, S., Berliner, J. A., Kirchgessner, T. G., and Lusis, A. J. (2006) Identification of inflammatory gene modules based on variations of human endothelial cell responses to oxidized lipids. *Proc. Natl. Acad. Sci. U.S.A.* **103,** 12741–12746
23. Furukawa, M., and Xiong, Y. (2005) BTB protein Keap1 targets antioxidant transcription factor Nrf2 for ubiquitination by the Cullin 3-Roc1 ligase. *Mol. Cell Biol.* **25,** 162–171
24. Creech, C. C., and Neumann, D. M. (2010) Changes to euchromatin on LAT and ICP4 following reactivation are more prevalent in an efficiently reactivating strain of HSV-1. *PLoS ONE* **5,** e15416
25. Shan, J., Fu, L., Balasubramanian, M. N., Anthony, T., and Kilberg, M. S. (2012) ATF4-dependent regulation of the JMJD3 gene during amino acid deprivation can be rescued in Atf4-deficient cells by inhibition of deacetylation. *J. Biol. Chem.* **287,** 36393–36403
26. Tietze, F. (1969) Enzymic method for quantitative determination of nanogram amounts of total and oxidized glutathione: applications to mammalian blood and other tissues. *Anal. Biochem.* **27,** 502–522
27. Han, J., Back, S. H., Hur, J., Lin, Y.-H., Gildersleeve, R., Shan, J., Yuan, C. L., Krokowski, D., Wang, S., Hatzoglou, M., Kilberg, M. S., Sartor, M. A., and Kaufman, R. J. (2013) ER-stress-induced transcriptional regulation increases protein synthesis leading to cell death. *Nat. Cell Biol.* **15,** 481–490
28. Oh-Hashi, K., Nomura, Y., Shimada, K., Koga, H., Hirata, Y., and Kiuchi, K. (2013) Transcriptional and post-translational regulation of mouse cation transport regulator homolog 1. *Mol. Cell Biochem.* **380,** 97–106
29. Kilberg, M. S., Shan, J., and Su, N. (2009) ATF4-dependent transcription mediates signaling of amino acid limitation. *Trends Endocrinol. Metab.* **20,** 436–443
30. Romanoski, C. E., Che, N., Yin, F., Mai, N., Pouldar, D., Civelek, M., Pan, C., Lee, S., Vakili, L., Yang, W.-P., Kayne, P., Mungrue, I. N., Araujo, J. A., Berliner, J. A., and Lusis, A. J. (2011) Network for activation of human endothelial cells by oxidized phospholipids: a critical role of heme oxygenase 1. *Circ. Res.* **109,** e27–41
31. Chérasse, Y., Maurin, A.-C., Chaveroux, C., Jousse, C., Carraro, V., Parry, L., Deval, C., Chambon, C., Fafournoux, P., and Bruhat, A. (2007) The p300/CBP-associated factor (PCAF) is a cofactor of ATF4 for amino acid-regulated transcription of CHOP. *Nucleic Acids Res.* **35,** 5954–5965
32. Siu, F., Bain, P. J., LeBlanc-Chaffin, R., Chen, H., and Kilberg, M. S. (2002) ATF4 is a mediator of the nutrient-sensing response pathway that activates the human asparagine synthetase gene. *J. Biol. Chem.* **277,** 24120–24127
33. Ohoka, N., Yoshii, S., Hattori, T., Onozaki, K., and Hayashi, H. (2005) TRB3, a novel ER stress-inducible gene, is induced via ATF4-CHOP pathway and is involved in cell death. *EMBO J.* **24,** 1243–1255
34. Teske, B. F., Fusakio, M. E., Zhou, D., Shan, J., McClintick, J. N., Kilberg, M. S., and Wek, R. C. (2013) CHOP induces activating transcription factor 5 (ATF5) to trigger apoptosis in response to perturbations in protein homeostasis. *Mol. Biol. Cell* **24,** 2477–2490
35. Wolfgang, C. D., Liang, G., Okamoto, Y., Allen, A. E., and Hai, T. (2000) Transcriptional autorepression of the stress-inducible gene ATF3. *J. Biol. Chem.* **275,** 16865–16870
36. Fu, L., and Kilberg, M. S. (2013) Elevated cJUN expression and an ATF/CRE site within the ATF3 promoter contribute to activation of ATF3 transcription by the amino acid response. *Physiol. Genomics* **45,** 127–137
37. Balasubramanian, M. N., Butterworth, E. A., and Kilberg, M. S. (2013) Asparagine synthetase: regulation by cell stress and involvement in tumor biology. *Am. J. Physiol. Endocrinol. Metab.* **304,** E789–99
38. Goebel, G., Berger, R., Strasak, A. M., Egle, D., Müller-Holzner, E., Schmidt, S., Rainer, J., Presul, E., Parson, W., Lang, S., Jones, A., Widschwendter, M., and Fiegl, H. (2012) Elevated mRNA expression of CHAC1 splicing variants is associated with poor outcome for breast and ovarian cancer patients. *Br. J. Cancer* **106,** 189–198
39. Galluzzi, L., De Santi, M., Crinelli, R., De Marco, C., Zaffaroni, N., Duranti, A., Brandi, G., and Magnani, M. (2012) Induction of endoplasmic reticulum stress response by the indole-3-carbinol cyclic tetrameric derivative CTet in human breast cancer cell lines. *PLoS ONE* **7,** e43249
40. Joo, N. E., Ritchie, K., Kamarajan, P., Miao, D., and Kapila, Y. L. (2012) Nisin, an apoptogenic bacteriocin and food preservative, attenuates HNSCC tumorigenesis via CHAC1. *Cancer Med.* **1,** 295–305
41. Selvik, L.-K., Fjeldbo, C. S., Flatberg, A., Steigedal, T. S., Misund, K., Anderssen, E., Doseth, B., Langaas, M., Tripathi, S., Beisvag, V., Lægreid, A., Thommesen, L., and Bruland, T. (2013) The duration of gastrin treatment affects global gene expression and molecular responses involved in ER stress and anti-apoptosis. *BMC Genomics* **14,** 429
42. Magne, L., Blanc, E., Legrand, B., Lucas, D., Barouki, R., Rouach, H., and Garlatti, M. (2011) ATF4 and the integrated stress response are induced by ethanol and cytochrome P450 2E1 in human hepatocytes. *J. Hepatol.* **54,** 729–737
43. Zhang, W., Li, H., Cheng, G., Hu, S., Li, Z., and Bi, D. (2008) Avian influenza virus infection induces differential expression of genes in chicken kidney. *Res. Vet. Sci.* **84,** 374–381
44. Tang, C., Lan, D., Zhang, H., Ma, J., and Yue, H. (2013) Transcriptome analysis of duck liver and identification of differentially expressed transcripts in response to duck hepatitis A virus genotype C infection. *PLoS ONE* **8,** e71051
45. Yasuda, M., Tanaka, Y., Ryu, M., Tsuda, S., and Nakazawa, T. (2014) RNA sequence reveals mouse retinal transcriptome changes early after axonal injury. *PLoS ONE* **9,** e93258